Simultaneous visualization of the extracellular and cytoplasmic domains of the epidermal growth factor receptor

Li-Zhi Mi[1], Chafen Lu[1], Zongli Li[2], Noritaka Nishida[3], Thomas Walz[2] & Timothy A Springer[1]

To our knowledge, no structural study to date has characterized, in an intact receptor, the coupling of conformational change in extracellular domains through a single-pass transmembrane domain to conformational change in cytoplasmic domains. Here we examine such coupling, and its unexpected complexity, using nearly full-length epidermal growth factor receptor (EGFR) and negative-stain EM. The liganded, dimeric EGFR ectodomain can couple both to putatively active, asymmetrically associated kinase dimers and to putatively inactive, symmetrically associated kinase dimers and monomers. Inhibitors that stabilize the active or inactive conformation of the kinase active site, as well as mutations in the kinase dimer interface and a juxtamembrane phosphorylation site, shift the equilibrium among the three kinase association states. This coupling of one conformation of an activated receptor ectodomain to multiple kinase-domain arrangements reveals previously unanticipated complexity in transmembrane signaling and facilitates regulation of receptor function in the juxtamembrane and cytoplasmic environments.

Crystallographic studies have offered remarkable insights into conformational changes that occur in the isolated extracellular and cytoplasmic domains of receptors with single-pass transmembrane domains, such as EGFR[1–3]. The extracellular domain of EGFR adopts a conformation in the absence of ligand with an intramolecular tether between domains II and IV[4,5]. After binding of ligand, the intramolecular tether is broken, the arrangement of domains I–IV becomes more elongated and the receptor dimerizes through a newly exposed interface[1,2]. The EGFR kinase domain has little catalytic activity unless dimerized through an asymmetric interface[3,6]. Association of two kinase domains in an asymmetric dimer, in which the C-lobe of one kinase domain interacts with the N-lobe of the other, stabilizes the latter in a conformation with elevated catalytic activity[3]. In addition, the intracellular juxtamembrane region contributes to kinase activation by participating in the asymmetric contacts[6,7].

Distinct, inactive conformations of the EGFR and ErbB3 kinase domains have been visualized in crystal lattices containing symmetric dimeric interfaces[6,8]. Nonetheless, little is known about the coupling between ligand binding and intracellular signaling in receptors with single-pass transmembrane domains. Even the assumption that binding of ligand dictates a specific relative orientation between monomers that is transmitted to induce a specific, active orientation between the cytoplasmic domains is untested. Also untested is the common assumption of 1:1 linkage between active states of the extracellular and kinase domains. However, it is known that

regulation of receptor tyrosine kinases is complex and includes phosphorylation of the juxtamembrane region[9–11].

Here we present negative-stain EM data on nearly full-length EGFR. The unliganded, monomeric receptor adopts a tethered ectodomain conformation. In liganded, dimeric receptor, the asymmetric kinase dimer coexists with a symmetric kinase dimer and a monomeric kinase state. Inhibitors that stabilize the active or inactive conformation of the kinase active site, a mutation in the asymmetric interface, and mutations in the juxtamembrane region shift the equilibrium among the three kinase association states. This coupling of one conformation of an activated receptor ectodomain to multiple kinase-domain arrangements represents previously unanticipated complexity in transmembrane signaling and facilitates regulation of receptor function in the juxtamembrane and cytoplasmic environments.

RESULTS
Unliganded and liganded receptor
A human EGFR construct comprising the ecto-, transmembrane, juxtamembrane and kinase domains, and lacking the autophosphorylation tail (residues 999–1186), was affinity-purified in Triton X-100, treated (or not) with epidermal growth factor (EGF), and subjected to size fractionation in 0.2 mM dodecylmaltoside (DDM) (**Fig. 1a**). The unliganded receptor eluted as a symmetric peak with a monomeric Stokes radius of 5.9 nm (**Fig. 1a**). The EGF-treated sample was largely dimeric, with a Stokes radius of 7.6 nm (**Fig. 1a**). Peak fractions were subjected

Figure 1 Unliganded EGFR adopts a monomeric tethered conformation. (**a**) Superose 6 gel filtration chromatograms of EGFR with the indicated pretreatments. D, dimer; M, monomer. In preparations with EGF, the amount of monomer present varied in independent preparations with the same mutation or drug, and thus variations in monomer content in the profiles in **a** are not meaningful. (**b**) Representative EM class averages of unliganded EGF receptors. (**c**) The ectodomain after masking. (**d**) Bottom, the best cross-correlating projections from the unliganded ectodomain crystal structure. Top, enlarged ribbon diagrams in same orientation. (**e**) The best correlating projections with a monomer from the dimeric, liganded ectodomain crystal structure. Cross-correlation coefficients are shown below the projections. Scale bars, 10 nm.
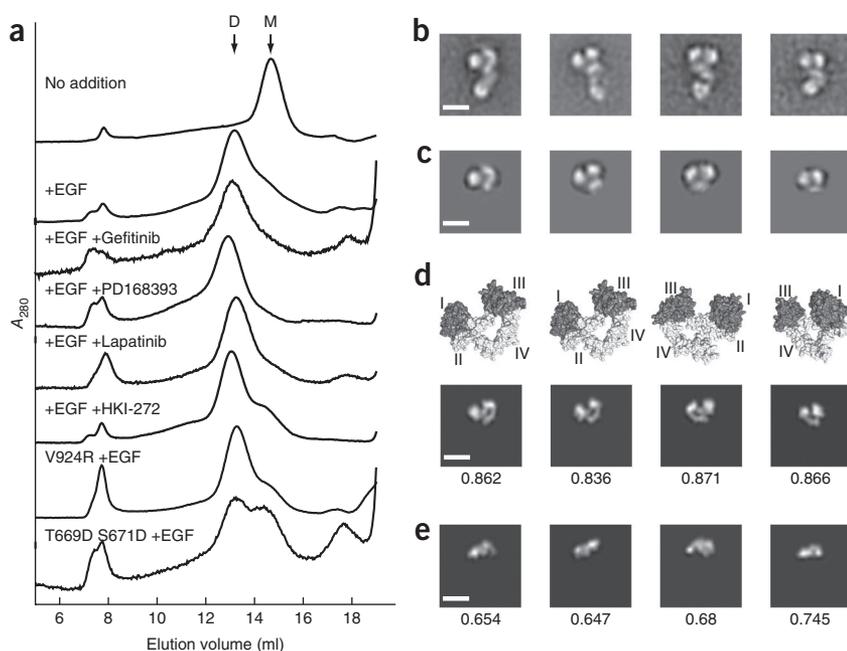
to negative-stain EM and iterative *K*-means classification and multireference alignment of 3,000–13,000 particles into 30–50 classes (**Supplementary Figs. 1–9**).

For the monomeric receptor, almost all class averages showed three major densities (**Fig. 1b** and **Supplementary Fig. 1**). A mask was drawn around the putative ectodomain (**Fig. 1c**), and it was cross-correlated with projections from the 20-Å-resolution filtered crystal structures of the tethered, monomeric ectodomain (**Fig. 1d**) and of the monomer from the EGF-bound dimer (**Fig. 1e**). The shape of the best-correlating projections from the tethered ectodomains corresponded well to the EM averages, with high cross-correlation coefficients (**Fig. 1d**). By contrast, the ectodomain monomer from the dimeric EGFR–EGF complex structure fit poorly (**Fig. 1e**). The same results were found for all 23 class averages, with good separation between the ecto- and kinase domains (**Supplementary Fig. 10**). Thus, detergent-soluble human EGFR monomers adopt a tethered conformation similar to that seen in crystals[4,5]. The relative orientation between the ectodomain and kinase domain was variable, and these domains thus appear to be uncoupled.

Ligand-bound dimeric receptors

The dimeric EGFR complex with EGF (**Fig. 2**) yielded distinct densities for the ectodomain (upper densities in **Fig. 2a,b**) and kinase domain (lower densities in **Fig. 2a,b**). The ectodomain contains two kidney-shaped densities with their concave sides facing each other, forming an overall heart shape. The masked ectodomain (**Fig. 2c,d**) shows excellent cross-correlation with crystal structure projections of the EGF-liganded, dimeric EGFR ectodomain (**Fig. 2e,f**)[12,13].

Two strikingly different kinase dimer association states were seen (**Fig. 2a,b**). One kinase dimer was ring-like or globular (**Fig. 2b**). The other kinase dimer was rod-like and was associated through one end with the ectodomain (**Fig. 2a**). The rod-like shape and association through one end require that the kinase domains be asymmetrically associated, as a symmetry axis parallel to the long axis of a rod is not possible for two globular domains. In better-resolved class averages, the rod had a perpendicular or diagonal orientation with respect to the ectodomain, and a smaller density was present corresponding to domain IV and the transmembrane domain (**Fig. 2a**).

Both symmetric and asymmetric kinase dimers have been seen in crystals[3]. We cross-correlated the kinase moiety (**Fig. 2g,h**) with multiple crystallographic kinase dimers (**Supplementary Fig. 11**).

The rod-like, asymmetric kinase dimer (**Fig. 2g**) cross-correlated well to the asymmetric dimer (**Fig. 2i,m**); this dimer is physiologically relevant to stabilizing the active conformation of the EGFR kinase domain[3]. In this asymmetric dimer, the C-lobe of one monomer contacts the N-lobe of the other monomer, allosterically activating it (**Fig. 2o**); the other C-lobe and N-lobe are at opposite ends of the dimer, giving rise to the elongated shape. We used cross-correlation with masked class averages (**Fig. 2c,d,g,h**) to determine the relative positions and two-dimensional orientations of the ectodomain and kinase-domain crystal structures, and these structures are shown as ribbon diagrams enlarged relative to the class averages while maintaining spatial relationships (**Fig. 2m,n**). All 12 class averages with asymmetric-like dimers cross-correlated markedly better with the asymmetric dimer than with six different symmetric dimers (**Supplementary Fig. 11a**). In contrast, the class averages with symmetric-like dimers (**Fig. 2b,h**) cross-correlated markedly better with symmetric dimers (**Fig. 2l,n** and **Supplementary Fig. 11a**).

Effect of mutations

The V924R mutation in the asymmetric kinase dimer interface (star, **Fig. 2o**) abolishes activation of EGFR kinase activity and formation of asymmetric dimers in crystal lattices[3,6]. EGF dimerized the V924R mutant EGFR (**Fig. 1a**); however, the dimers lacked autophosphorylation activity (**Supplementary Fig. 12**). Furthermore, although the dimeric ectodomain in the presence of EGF (**Fig. 3a,b**) was indistinguishable from the wild-type EGFR, no asymmetric, rod-like kinase dimer densities were present (**Fig. 3** and **Supplementary Figs. 3** and **11**). Instead, the kinase domains were either unassociated with one another (**Fig. 3a,c**) or symmetrically associated (**Fig. 3b,d**).

Several sites of serine and threonine phosphorylation in the EGFR juxtamembrane region have been found to regulate tyrosine kinase activity[11,14,15]. We tested effects of two mutations on kinase association state by EM and autophosphorylation, and we observed an effect of T669D S671D but little effect of T654D on association state in EM (**Fig. 3e,f** and **Supplementary Figs. 5** and **11**) or on autophosphorylation (**Supplementary Fig. 12**). The T669D S671D mutation eliminated the asymmetric kinase dimer; only unassociated monomers and symmetric kinase dimers were evident (**Fig. 3e–h**).
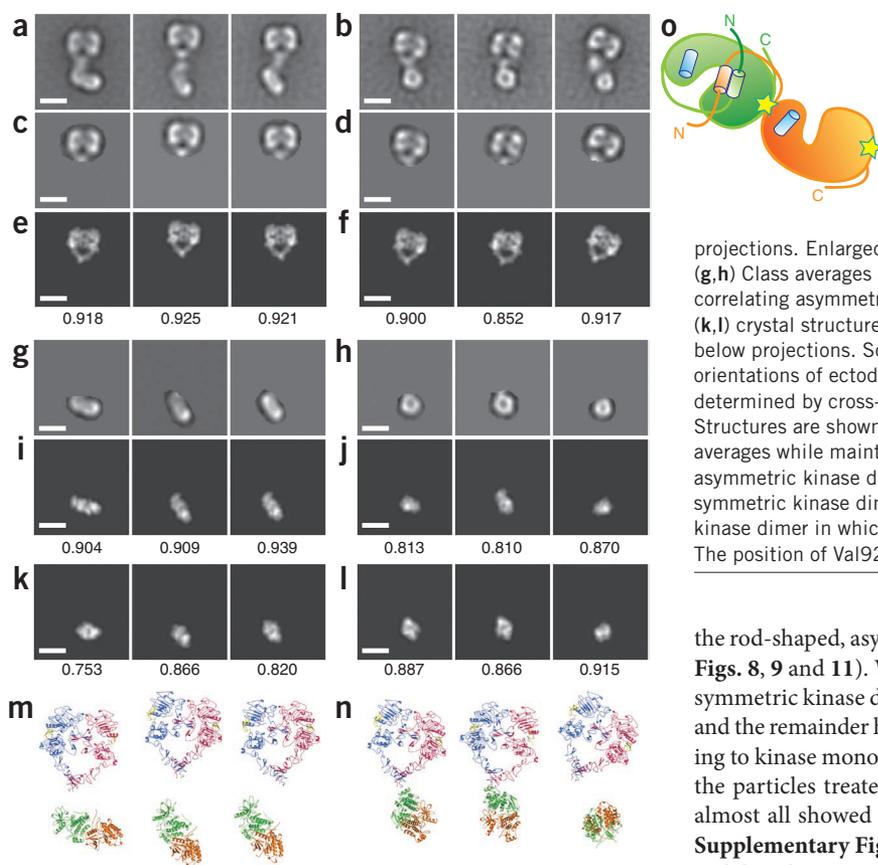
Figure 2 The liganded EGF receptor ectodomain can link to multiple kinase-domain dimerization states. (**a,b**) Representative EM class averages of EGF-bound receptors with asymmetric (**a**) or symmetric (**b**) kinase-domain dimers, with masked regions and cross-correlations for each average shown below in **c**–**n**. (**c,d**) Class averages after masking of all but the ectodomain. (**e,f**) Best-correlating ectodomain projections. Enlarged ribbon diagrams are shown in upper parts of **m,n**. (**g,h**) Class averages after masking of all but the kinase domain. (**i**–**l**) Best-correlating asymmetric kinase domain (**i,j**) and symmetric kinase domain (**k,l**) crystal structure projections. Cross-correlation scores are shown below projections. Scale bars, 10 nm. (**m,n**) Positions and two-dimensional orientations of ectodomain and kinase-domain crystal structures, determined by cross-correlation with masked class averages in **c,d,g,h**. Structures are shown as ribbon diagrams enlarged relative to the class averages while maintaining spatial relationships. The better-correlating asymmetric kinase dimer is shown in **m**, and the better-correlating symmetric kinase dimer in **n**. (**o**) Schematic diagram of the asymmetric kinase dimer in which one kinase (green) activates the other (orange). The position of Val924 is marked with a star. Modified from reference 6.

Active site inhibitors

Inactive and active conformations of the kinase domain, with the α-C helix swung out or swung in, respectively, can be stabilized by two distinct classes of inhibitors that bind to the active site[3,16–19]. PD168393, an irreversible inhibitor, and gefitinib, a reversible inhibitor, stabilize the active conformation of the kinase domain relative to the inactive conformation. We found that the asymmetric kinase dimer predominated in the EGFR–EGF complex in the presence of both inhibitors, with small amounts of the symmetric dimer; in gefitinib, there were also some unassociated kinase monomers (**Fig. 4** and **Supplementary Figs. 6, 7** and **11**). Notably, each of the inhibitors that stabilized the active kinase conformation increased the proportion of particles with the asymmetric kinase dimer and decreased the proportion with the symmetric dimer (**Fig. 4k**).

Markedly different results were obtained with HKI-272, an irreversible inhibitor, and lapatinib, a reversible inhibitor (**Fig. 5**), both of which stabilize the kinase in an inactive conformation by pushing the α-C helix out of the ATP-binding pocket[16,20]. Receptors treated with EGF plus lapatinib or HKI-272 (**Fig. 1a**) showed the dimeric ectodomain, but not

the rod-shaped, asymmetric kinase dimer (**Fig. 5** and **Supplementary Figs. 8, 9** and **11**). With lapatinib, 31% of particles had a ring-shaped symmetric kinase dimer (**Figs. 4k** and **5a** and **Supplementary Fig. 8**), and the remainder had two separate intracellular densities corresponding to kinase monomers (**Fig. 5b** and **Supplementary Fig. 9**). Among the particles treated with EGF and the covalent inhibitor HKI-272, almost all showed the kinase-dissociated state (**Figs. 4k** and **5c** and **Supplementary Fig. 9**). The distances between the kinase monomers and the relative orientations between them and the ectodomains varied across different class averages (**Fig. 5b,c**).

DISCUSSION

We have provided the first structures, to our knowledge, that simultaneously reveal the conformations of the ectodomain and the cytoplasmic domain in a receptor that has separate domains connected by a single-pass transmembrane domain. The unliganded EGFR was largely monomeric and showed the tethered, autoinhibited conformation of the extracellular domain seen in crystal structures[4,5]. The EGF-liganded receptor was largely dimeric and showed the dimeric

Figure 3 Mutational disruption of the asymmetric kinase dimer. (**a,b**) Representative class averages of EGFR V924R mutant in complex with EGF with unassociated kinase monomers (**a**) or symmetric kinase dimers (**b**). (**c,d**) Positions and two-dimensional orientations of ectodomain and kinase-domain crystal structures as in **Figure 2m,n**, determined using masked class averages in **a,b**. (**e,f**) Representative class averages of EGFR T669D S671D mutant in complex with EGF with unassociated kinase monomers (**e**) or symmetric kinase dimers (**f**). (**g,h**) Positions and two-dimensional orientations of ectodomain and kinase-domain crystal structures as in **Figure 2m,n**, determined using masked class averages from **e,f** as described in **Figure 2**. Scale bars, 10 nm.

Figure 4 Kinase inhibitors gefitinib and PD168393 cooperate with EGF in promoting the asymmetric kinase dimer. (**a**,**b**) Representative class averages of EGFR in complex with EGF and gefitinib or PD168393. Representative asymmetric dimeric (1), symmetric dimeric (2) and unassociated kinase domains (3) are shown. (**c**,**d**) The kinase domain after masking. (**e**–**j**) Best-correlating projections with asymmetric (**e**,**f**) and symmetric dimers (**g**,**h**) from kinase crystal structure. Cross-correlation scores are shown below each projection. Scale bars, 10 nm. (**i**,**j**) Positions and two-dimensional orientations of ectodomain and kinase-domain crystal structures determined using masked class averages as in **Figure 2**. (**k**) Fraction of asymmetric-like kinase dimers, symmetric-like kinase dimers and kinase monomers in the presence of EGF and indicated inhibitors or mutations, calculated using all class averages with well-resolved kinase domains and the number of particles in each class average. WT, wild-type.

conformation of the ectodomain as well as two distinct dimeric states and one unassociated state of the kinase domain.

Together with crystal structures[1–6], our results suggest that two types of kinase-domain conformation exist in dimeric EGF–EGFR complexes: inactive and active conformations, present in symmetric and asymmetric kinase-domain dimers, respectively. A third, unassociated kinase-domain state observed in presence of mutations and inhibitors may hint at yet a third conformational state of the kinase domain. Relative to our previous EM studies[12], the structural detail present in the kinase-domain moiety here was greatly improved owing to the use of the lowest DDM concentration that enables fractionation by gel filtration (and that also preserves kinase activity[12]) and because only 5–7 h elapsed between cell lysis and application of purified EGFR to EM grids. However, an important caveat is that although the nonionic detergents used here probably preserve overall features such as the predicted α-helices in the transmembrane and juxtamembrane domains, they differ in curvature and charge distribution from lipid bilayers and are imperfect membrane mimics.
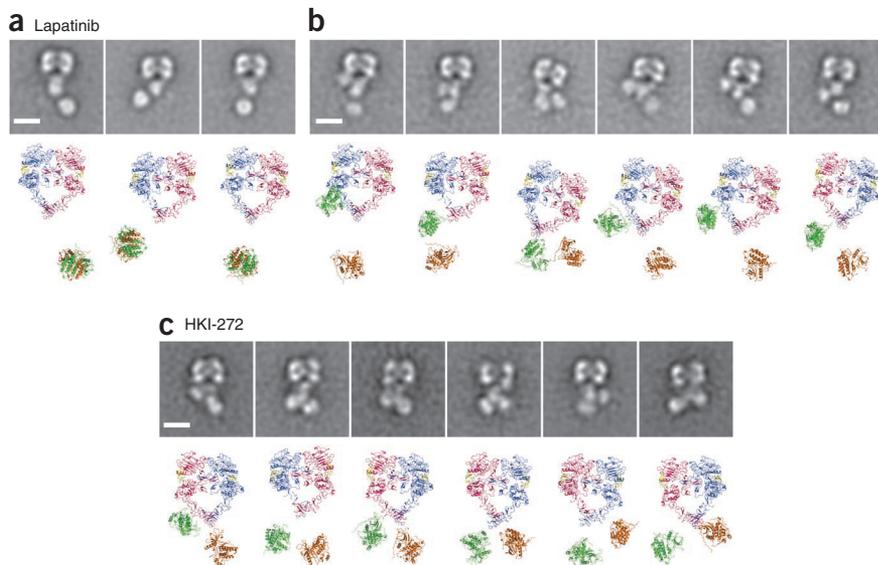
Figure 5 Effect of the inhibitors lapatinib and HKI-272 on kinase-domain dimerization. (**a**,**b**) Representative class averages of EGFR in complex with EGF and lapatinib as symmetric kinase dimers (**a**) or unassociated kinase monomers (**b**). (**c**) Top, representative class averages of EGFR in complex with EGF and HKI-272. Scale bars, 10 nm. Bottom, positions and two-dimensional orientations of ectodomain and kinase-domain crystal structures, as determined using masked class averages as in **Figure 2**.

A rod-like kinase-domain dimer connected at one end to the EGFR ectodomain demonstrated asymmetric dimerization of the kinase domains and cross-correlated well with an asymmetric dimer seen in crystals[3]. Mutagenesis has shown that kinase association through the asymmetric interface is closely linked to activation of receptor tyrosine kinase activity[3]; here mutation also blocked formation of the asymmetric kinase dimer seen in EM. Our results in nearly full-length, intact EGF receptors directly confirm the remarkable idea, previously suggested on the basis of crystal structures of the isolated extracellular and kinase domains, that the symmetric, liganded ectodomain dimer is linked to an asymmetric kinase-domain dimer (refs. 3,6). In better-resolved class averages, the long axes of the ectodomain and asymmetric kinase dimer approached perpendicular. This orientation would place both kinase domains in proximity to the inner face of the plasma membrane. A similar orientation of the kinase domains has been proposed on the basis of crystal, mutagenesis and modeling studies[6].

We also observed both a distinct, symmetric-like kinase dimer that cross-correlated well with symmetric dimers seen in crystal structures and also an unassociated, monomeric kinase state. The inhibitors PD168393 and gefitinib, known to favor the active kinase-domain conformation[19] increased the proportion of asymmetric kinase dimer. Conversely, two inhibitors, lapatinib and HKI-272, that stabilize the kinase active site in an inactive conformation abolished the asymmetric kinase dimer. In the presence of the latter inhibitors, the dimeric ectodomain was either associated with the symmetric kinase dimer and unassociated kinase monomers (lapatinib) or associated almost exclusively with unassociated kinase monomers (HKI-272).

In all class averages with dimeric ectodomains and kinase domains, the positions of the ectodomains and kinase domains in projections were consistent with their being on opposite sides of an imaginary plasma-membrane projection. However, in class averages with monomeric kinase domains, the positions of kinase domains were much more variable and included nonphysiologic positions proximal to the ectodomain. The two kinase domains were also sometimes distant from each other. These results are consistent not only with a lack of dimerization of the kinase domains but also with a lack of dimerization of the 34-residue juxtamembrane linkers between the transmembrane and kinase domains. Notably, despite the absence of a plasma-membrane barrier, the kinase domains in asymmetric and symmetric dimers oriented in two-dimensional projections on the opposite side of a putative transmembrane and juxtamembrane domain density from the ectodomain. This may reflect shortening of the juxtamembrane region by its participation in the kinase-domain dimer interface and, in the case of the asymmetric kinase dimer, additional antiparallel interactions between the N-terminal segments of the juxtamembrane regions that potentiate dimerization[6].

Our observation that one overall extracellular domain conformation can couple to multiple intracellular domain arrangements contrasts with a previously widely held notion: that ligand binding would induce a specific, dimeric conformation of the extracellular domain, which in turn would be transmitted through the membrane to promote a specific, dimeric conformation of the intracellular domain. However, the lack of a requirement for a fixed orientation between the EGFR ectodomain and kinase domain is consistent with early evidence for triggering by antibodies to different ectodomain epitopes, by truncation of the ectodomain in the V-*erb*B avian oncogene and by insertion in the ectodomain (see ref. 21 and references therein). Furthermore, we have found that no specific transmembrane α-helical interface is required for EGFR activation[13].

Linking one ligand-bound ectodomain conformation with multiple kinase-domain arrangements provides more scope for regulation of EGFR activity. Regulation is known to be highly complex and to operate on many levels, including phosphorylation of threonine and serine residues in the juxtamembrane region[9,10,22–25]. Furthermore, activity is regulated through binding of inhibitory factors such as Mig-6 (refs. 22,23), ubiquitination[26] and internalization followed by degradation or recycling[24,25]. These processes might alter the populations of the three different kinase association states visualized here or select for states. We have found that mutation to aspartate of two juxtamembrane residues known to be phosphorylated *in vivo*, Thr669 and Ser671 (refs. 14,15), inhibits kinase activity and asymmetric dimer formation; double mutation to alanine of these residues has also been reported to be inhibitory[15]. Further mutations showed that Ser671, but not Thr669, is required for kinase activity, and that both S671A and S671D mutations are inhibitory (**Supplementary Fig. 12**). Notably, the side chain of Ser671, but not that of Thr669, is in the asymmetric kinase dimer interface[6,7]. Furthermore, a side chain hydrogen bond between Ser671 of one kinase monomer and Asp950 of the other monomer[7] is consistent with inhibition by both the S671A mutation and the phosphomimetic S671D mutation, and predicts inhibition by phosphorylation *in vivo*.

Our study also has implications for small-molecule therapeutics targeting EGFR, several of which, including lapatinib, are approved for treatment of cancer[27]. All of these bind to the active site and block kinase activity. However, we have shown that inhibitors with different effects on the conformation around the kinase active site have very different effects on the state of association of the kinase domain in liganded receptors. These different association states could have distinct downstream effects, such as on receptor internalization and degradation, with important clinical consequences.

METHODS

Methods and any associated references are available in the online version of the paper at http://www.nature.com/nsmb/.

Note: Supplementary information is available on the Nature Structural & Molecular Biology website.

AUTHOR CONTRIBUTIONS
L.-Z.M. prepared constructs, designed and carried out experiments, and wrote the manuscript. C.L. prepared constructs, designed and carried out experiments, and discussed the writeup. N.N. performed early EM experiments. Z.L. trained N.N. and L.-Z.M., and maintained and supervised the EM facility. T.W. discussed and supervised EM experiments and strategy, wrote the manuscript, and helped respond to referees. T.A.S. designed the overall experimental approach, supervised experiments, wrote the manuscript and responded to referees.

1. Ogiso, H. *et al.* Crystal structure of the complex of human epidermal growth factor and receptor extracellular domains. *Cell* **110**, 775–787 (2002).
2. Garrett, T.P. *et al.* Crystal structure of a truncated epidermal growth factor receptor extracellular domain bound to transforming growth factor α. *Cell* **110**, 763–773 (2002).
3. Zhang, X., Gureasko, J., Shen, K., Cole, P.A. & Kuriyan, J. An allosteric mechanism for activation of the kinase domain of epidermal growth factor receptor. *Cell* **125**, 1137–1149 (2006).
4. Li, S. *et al.* Structural basis for inhibition of the epidermal growth factor receptor by cetuximab. *Cancer Cell* **7**, 301–311 (2005).
5. Cho, H.S. & Leahy, D.J. Structure of the extracellular region of HER3 reveals an interdomain tether. *Science* **297**, 1330–1333 (2002).

6. Jura, N. *et al.* Mechanism for activation of the EGF receptor catalytic domain by the juxtamembrane segment. *Cell* **137**, 1293–1307 (2009).
7. Red Brewer, M. *et al.* The juxtamembrane region of the EGF receptor functions as an activation domain. *Mol. Cell* **34**, 641–651 (2009).
8. Shi, F., Telesco, S.E., Liu, Y., Radhakrishnan, R. & Lemmon, M.A. ErbB3/HER3 intracellular domain is competent to bind ATP and catalyze autophosphorylation. *Proc. Natl. Acad. Sci. USA* **107**, 7692–7697 (2010).
9. Hunter, T., Ling, N. & Cooper, J.A. Protein kinase C phosphorylation of the EGF receptor at a threonine residue close to the cytoplasmic face of the plasma membrane. *Nature* **311**, 480–483 (1984).
10. Morrison, P., Takishima, K. & Rosner, M.R. Role of threonine residues in regulation of the epidermal growth factor receptor by protein kinase C and mitogen-activated protein kinase. *J. Biol. Chem.* **268**, 15536–15543 (1993).
11. Thiel, K.W. & Carpenter, G. Epidermal growth factor receptor juxtamembrane region regulates allosteric tyrosine kinase activation. *Proc. Natl. Acad. Sci. USA* **104**, 19238–19243 (2007).
12. Mi, L.Z. *et al.* Functional and structural stability of the epidermal growth factor receptor in detergent micelles and phospholipid nanodiscs. *Biochemistry* **47**, 10314–10323 (2008).
13. Lu, C. *et al.* Structural evidence for loose linkage between ligand binding and kinase activation in the epidermal growth factor receptor. *Mol. Cell. Biol.* **30**, 5432–5443 (2010).
14. Heisermann, G.J. & Gill, G.N. Epidermal growth factor receptor threonine and serine residues phosphorylated in vivo. *J. Biol. Chem.* **263**, 13152–13158 (1988).
15. Heisermann, G.J. *et al.* Mutational removal of the Thr669 and Ser671 phosphorylation sites alters substrate specificity and ligand-induced internalization of the epidermal growth factor receptor. *J. Biol. Chem.* **265**, 12820–12827 (1990).
16. Wood, E.R. *et al.* A unique structure for epidermal growth factor receptor bound to GW572016 (Lapatinib): relationships among protein conformation, inhibitor off-rate, and receptor activity in tumor cells. *Cancer Res.* **64**, 6652–6659 (2004).
17. Stamos, J., Sliwkowski, M.X. & Eigenbrot, C. Structure of the epidermal growth factor receptor kinase domain alone and in complex with a 4-anilinoquinazoline inhibitor. *J. Biol. Chem.* **277**, 46265–46272 (2002).
18. Yun, C.H. *et al.* Structures of lung cancer-derived EGFR mutants and inhibitor complexes: mechanism of activation and insights into differential inhibitor sensitivity. *Cancer Cell* **11**, 217–227 (2007).
19. Eck, M.J. & Yun, C.H. Structural and mechanistic underpinnings of the differential drug sensitivity of EGFR mutations in non-small cell lung cancer. *Biochim. Biophys. Acta* **1804**, 559–566 (2010).
20. Yun, C.H. *et al.* The T790M mutation in EGFR kinase causes drug resistance by increasing the affinity for ATP. *Proc. Natl. Acad. Sci. USA* **105**, 2070–2075 (2008).
21. Sorokin, A. Activation of the EGF receptor by insertional mutations in its juxtamembrane regions. *Oncogene* **11**, 1531–1540 (1995).
22. Hackel, P.O., Gishizky, M. & Ullrich, A. Mig-6 is a negative regulator of the epidermal growth factor receptor signal. *Biol. Chem.* **382**, 1649–1662 (2001).
23. Zhang, X. *et al.* Inhibition of the EGF receptor by binding of MIG6 to an activating kinase domain interface. *Nature* **450**, 741–744 (2007).
24. Carpenter, G. & Cohen, S. 125I-labeled human epidermal growth factor. Binding, internalization, and degradation in human fibroblasts. *J. Cell Biol.* **71**, 159–171 (1976).
25. Honegger, A.M. *et al.* Point mutation at the ATP binding site of EGF receptor abolishes protein-tyrosine kinase activity and alters cellular routing. *Cell* **51**, 199–209 (1987).
26. Huang, F., Kirkpatrick, D., Jiang, X., Gygi, S. & Sorkin, A. Differential regulation of EGF receptor internalization and degradation by multiubiquitination within the kinase domain. *Mol. Cell* **21**, 737–748 (2006).
27. Geyer, C.E. *et al.* Lapatinib plus capecitabine for HER2-positive advanced breast cancer. *N. Engl. J. Med.* **355**, 2733–2743 (2006).

ONLINE METHODS

Materials. Recombinant human EGF and thin-carbon-coated EM grids were from Pepro Tech and Pacific Grid-Tech, respectively. Triton X-100 and *n*-dodecyl-β-D-maltoside (DDM) were from Anatrace.

Protein expression and purification. EGFRΔ998 (residues 1–998) was subcloned into the ExpressTag-1 vector, which includes C-terminal streptavidin-binding peptide and histidine tags[12]. Protein expression and purification were as described[12] except that 0.2 mM DTT was added to all purification and column chromatography buffers, and the DDM concentration was lowered to 0.2 mM.

Affinity-purified EGFRΔ998 (wild-type or mutant) was treated with or without 20 μM EGF and kinase inhibitors at 100 μM for 5 min on ice before fractionation on Superose 6 HR equilibrated with 20 mM Tris pH 8.0, 200 mM NaCl, 1 mM EDTA, 0.2 mM DTT and 0.2 mM DDM. We made the stock solution of 100 μM EGF by dissolving lyophilized EGF in deionized water, and the stock solution of 10 mM kinase inhibitor by dissolving inhibitor in DMSO. The peak fraction corresponding to either monomeric unliganded receptor or EGF-bound dimeric receptor was collected and immediately applied to EM grids for negative staining. As lapatinib and gefitinib are reversible kinase inhibitors, in tests of these compounds 100 μM of inhibitor was also added to the sample before negative staining.

Negative staining and EM image collection. In our previous study, after the sample was applied to a glow-discharged thin-carbon-coated grid, the excess sample was blotted off and the grid was immediately washed 2–4 times with water[12]. With such washing, most particles have the kinase domain in close proximity to the ectodomain. Uranyl formate is also a fixative. Better separation between the ecto- and kinase domains was achieved when washing was omitted and samples were stained (and in effect also fixed and washed) four times with four droplets of 0.75% (w/v) uranyl formate. After each staining, the grid was blotted on the edge with a filter paper to remove excess stain. Next, the grid was floated on a droplet of uranyl formate for 20 s. After blotting with a filter paper, the grid was air-dried and stored in a grid storage box.

EM images were collected with a Tecnai T12 microscope (FEI) equipped with a LaB$_6$ filament and operated at an acceleration voltage of 120 kV. Images were recorded on imaging plates using low-dose procedures at 67,000× magnification and a defocus of –1.5 μm. Imaging plates were read out with an imaging plate scanner (DITABIS Digital Biomedical); the pixel size at the specimen level was 4.5 Å.

Image processing. Particles were interactively picked using BOXER in EMAN[28]. Grid location coordinates were converted to SPIDER[29] format and used in windowing particles to create a boxed image stack. Each image in the stack was normalized to a mean intensity of 0 and s.d. of 50. Normalized images were subjected to ten iterations of centering, multivariate statistical analysis, *K*-means classification, class averaging and multireference alignment, with the class averages used as input references for multireference alignment in the next iteration. Changes were made from a previous study[12] that improved the accuracy of alignment and classification. In *K*-means classification, the seeds were randomly selected rather than sequentially picked from the stack. Instead of rotational search, a combined translational and rotational search was used to align particles in the multireference alignment step.

Cross-correlation with crystal structure projections. For cross-correlation, crystal structures were inflated by 10%, Fourier-transformed, filtered to 20 Å with a Butterworth low-pass filter and transformed back. Evenly spaced projections were calculated at 4° intervals and subjected to ten cycles of alignment with masked EM class averages. The cross-correlation coefficient is reported for the most similar crystal structure projection.

Asymmetric interface, phosphorylation site mutations and autophosphorylation. EGFR juxtamembrane mutations were introduced into wild-type receptor with a protein C tag at the C terminus[13]. Mutant and wild-type receptors were transiently expressed in 293T cells. Cells treated with or without EGF for 5 min were lysed with 1% (v/v) Triton X-100. Duplicate samples were subjected to western blotting, and total expression and autophosphorylation were quantified with protein C and 4G10 phosphotyrosine antibodies, respectively[13].

28. Ludtke, S.J., Baldwin, P.R. & Chiu, W. EMAN: semiautomated software for high-resolution single-particle reconstructions. *J. Struct. Biol.* **128**, 82–97 (1999).
29. Frank, J. *et al.* SPIDER and WEB: processing and visualization of images in 3D electron microscopy and related fields. *J. Struct. Biol.* **116**, 190–199 (1996).